Available online at www.sciencedirect.com
SCIENCE DIRECT®
Thin Solid Films 508 (2006) 182 – 185
thin solid films
www.elsevier.com/locate/tsf

Fabrication of nanocrystalline Si:H nanodot arrays with controllable porous alumina membranes

G.Q. Ding, M.J. Zheng, W.L. Xu, W.Z. Shen *

Laboratory of Condensed Matter Spectroscopy and Opto-Electronic Physics, Department of Physics, Shanghai Jiao Tong University, 1954 Hua Shan Road, Shanghai 200030, PR China

Available online 14 November 2005

Abstract

Based on the successful growth of hydrogenated nanocrystalline silicon (nc-Si:H) thin films with Si natural quantum dots (NQDs) of 3–6 nm in mean size, we have fabricated nc-Si:H artificial quantum nanodot (AQD) arrays on Si substrates by a low-cost and industrialized plasma-enhanced chemical vapor deposition technique through free-standing ultrathin porous alumina membranes (PAMs). In order to well control the morphology of the nc-Si:H AQD arrays, we have presented detailed information on the fabrication of PAMs with controllable thickness (100–1000 nm) and pore diameter (50–90 nm). In every nc-Si:H AQD, there are $\sim 10^2$ Si NQDs, and the sheet densities of nc-Si:H AQDs and Si NQDs are over 1×10^{10} cm^{-2} and 3×10^{11} cm^{-2}, respectively. The combination of the AQD fabrication through PAM masks with the Si NQDs in nc-Si:H provides us an easy and practical way for the realization of nc-Si:H based nanodevice arrays with true quantum size effects.

Keywords: Silicon; Nanostructrures; Anodic oxidation

1. Introduction

Nano-scale quantum dots (QDs), especially semiconductor QDs that exhibit unique properties based on their quantum size effects, are expected to be the building blocks of new functional materials as those used in devices such as single-electron transistors, high-density memories, semiconductor lasers, and tunneling diodes. Hydrogenated nanocrystalline silicon (nc-Si:H) thin films are composed approximately of 50% nanocrystalline Si (mean grain size 3–6 nm) and 50% amorphous Si (a-Si) tissues in the interface regions (thickness about 2–3 atomic spacing) among the grains [1]. The small natural quantum dots (NQDs) of nano-scale Si grains allow us to observe zero-dimensional (0D) electronic states with macroscopic contacts at high temperature, as demonstrated by the appearance of Coulomb staircases in ultrathin nc-Si/Si diodes [1] and nc-Si/a-SiO_2 systems [2]. Very recently, we have presented clear high temperature resonant tunneling through both the 0D and interfacial two-dimensional (2D) states in nc-Si:H/crystalline-Si (c-Si) heterostructures, based on the identification of confined low-dimensional carriers by magnetic-field-dependent Hall effect measurements [3]. The advantages of great fabrication simplicity and high operational temperature in Si NQDs pave the way for much wider applications of quantum confinement phenomena in nc-Si:H on desirable silicon substrates in the microelectronic industry.

Self-organized porous alumina membrane (PAM) is a highly ordered template, which has nanopore arrays with interpore spacing ranging from 50 to 400 nm, pore diameter from 20 to 200 nm, membrane thickness from 0.1 to 200 μm, and pore density as high as 10^{11} pores cm^{-2} [4]. The PAMs with these dimensions are suitable for both nanometric materials as well as photonic crystals. Using well-ordered PAMs as evaporation or etching masks, many nanostructured materials have been fabricated, including nanodots (made of Au, Ni, Co, Fe, Si and GaAs), nanopores (Si, GaAs and GaN), nanowires (ZnO) and nanotubes (silicon, carbon) [4]. It should be noted that, though many semiconductor nanodot arrays have been fabricated through the versatile PAM approach, these nanodot arrays are not systems with real quantum confinement effects due to the large nanodot size (normally over 25 nm). Furthermore, it is well known that the thickness and pore diameter of the PAMs play an important role in fabricating nanostructure materials.

* Corresponding author. Tel.: +86 21 54743242; fax: +86 21 54741040.
E-mail address: wzshen@sjtu.edu.cn (W.Z. Shen).

0040-6090/$ - see front matter © 2005 Elsevier B.V. All rights reserved.
doi:10.1016/j.tsf.2005.07.318

For example, hardly any growth of GaAs nanodots was observed when the PAM thickness exceeded 500 nm because the Ga atoms could not migrate to the substrate through the deep nanopores [5]. Therefore, only ultrathin PAMs (<1000 nm) can be employed in the fabrication of nanodots and nanopores, and the thickness should be as small as possible for the materials to go through the nanochannels easily. In order to well control the morphology of the deposited nanostructure materials, it is necessary to precisely adjust the thickness and pore diameter, which remain open questions.

In this paper, we report on the successful growth of highly ordered nc-Si:H artificial quantum dot (AQD) arrays on Si substrates for application in nanodevice arrays by a plasma-enhanced chemical vapor deposition (PECVD) technique through controllable PAMs with thickness of 100–1000 nm and pore diameter of 50–90 nm. The Si NQDs in the nc-Si:H AQDs will play a key role in the quantum size effects, while the uniform nc-Si:H AQDs establish the base for nc-Si:H nanodevice arrays with the spacing of the AQDs as a good electrical insulation.

2. Experimental details

The nc-Si:H thin films were deposited on n-type c-Si (100) substrates in a radio frequency (13.56 MHz) capacitive-coupled PECVD system from silane and hydrogen. Thin films with layer thickness of around 1.0 μm were deposited at a substrate temperature of 250 °C with total pressure of reactive gases of 1 Torr and percentage content of silane (SiH_4/SiH_4+H_2) of about 2%. In order to obtain nc-Si:H AQD arrays, PAMs were fabricated through a typical two-step anodization electrochemical procedure [6] with high-purity (99.999%) aluminum foil degreased in acetone as the anode in 0.3 M oxalic acid ($H_2C_2O_4$) electrolyte. The first anodization lasted for 2 h under the constant anodization voltage of 40 V and electrolyte temperature of 10 °C. The specimens were then immersed in a mixture of 6.0 wt.% H_3PO_4 and 1.8 wt.% H_2CrO_4 at 60 °C for 4 h to remove the alumina layers. The well-ordered concave patterns on the aluminum foil act as self-assembled masks for the second anodization. Ultrathin PAMs with different thickness were fabricated under different second anodization times and current densities, which were recorded by using a Keithley 2400 sourcemeter. The PAMs were separated from the Al substrates in a mixture solution of saturated $CuSO_4$ and HCl (38%), and transferred into a 5% H_3PO_4 solution for 30–60 min at 30 °C to remove the barrier layers and adjust the pore diameters. After several times washing in deionized water, the throughout free-standing PAMs were easily placed on the Si substrates, and the whole specimens dried for the PECVD growth. The nc-Si:H AQD arrays were fabricated by PECVD through the PAM masks under the same deposition conditions for the nc-Si:H thin films.

3. Results and discussion

Fig. 1(a) displays the microstructure of the nc-Si:H thin films under high-resolution transmission electron microscopy (HRTEM, Philips CM200FEG). We have marked by white lines some of the ordered domains (i.e., Si NQDs) embedded in the a-Si matrix with the average size of about 4 nm. In order to confirm that the as-prepared thin films are "really" composed of nc-Si:H, we have performed X-ray diffraction (XRD, Bruker AXS D8 Discover GADDS) and micro-Raman scattering [Jobin Yvon HR 800 with a spatial resolution of 0.7 μm in back-scattering configuration using an Ar^+ laser (514.5 nm)] measurements. The XRD result (Fig. 1(b)) shows the relatively sharp crystalline Si (111) diffraction peak and broad Gaussian amorphous component at the same position, together with the sharp (220) diffraction structure, corroborating the two-phase mixed nature and good quality of these nc-Si:H thin films. The average grain size of 3.6 nm can be calculated from the width of the (220) diffraction peak by Scherrer formula, which is consistent with the HRTEM result. The room-temperature micro-Raman scattering spectrum (Fig. 1(c)) displays the typical asymmetric lineshape of nc-Si:H with contributions from both the amorphous (dashed Gaussian curves, centered at 300, 380, 480 cm^{-1}, respectively) and crystalline (dotted Gaussian curve, centered at ~514 cm^{-1}) silicon components, where the crystallinity can be deduced to be 42.7% by means of the method in Ref. [7]. It is noted that the HRTEM result also reveals approximately of 50% Si NQDs and 50% interfacial a-Si tissues in the nc-Si:H thin films. The quantum size effects from the Si NQDs have been demonstrated through the appearance of Coulomb staircases in ultrathin nc-Si/Si diodes [1] and nc-Si/a-SiO_2 [2] systems, as well as high temperature resonant tunneling through both the 0D and interfacial 2D states in nc-Si:H/c-Si heterostructures [3].

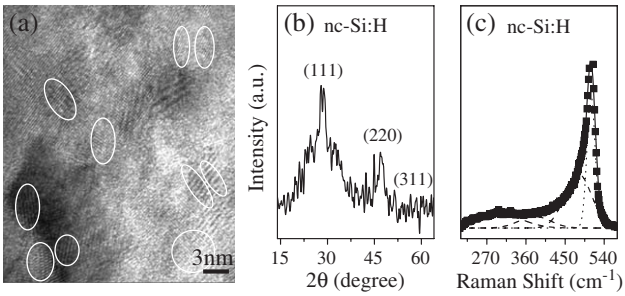

Fig. 1. (a) HRTEM image of a typical nc-Si:H thin film. Some of the ordered domains (i.e., Si NQDs) embedded in the amorphous Si matrix are marked by white lines. Room-temperature (b) XRD result and (c) micro-Raman scattering spectrum (filled squares) for the nc-Si:H thin film. The contribution of amorphous and crystalline Si has been extracted by the dashed and dotted curves, respectively, together with the overall results shown as the solid curve in (c).

In order to obtain nc-Si:H AQD arrays, ultrathin PAMs with controllable thickness and diameter were fabricated. The PAMs are fabricated through an electrochemical procedure, and the current–time characteristics of the second anodization are shown in Fig. 2(a). The current density firstly experiences a rapid drop within ~30 s, then increases slowly up to ~2 min, and finally remains basically constant as the anodization goes on. According to the variation of the current density with the anodization time, we can define regions in which the current

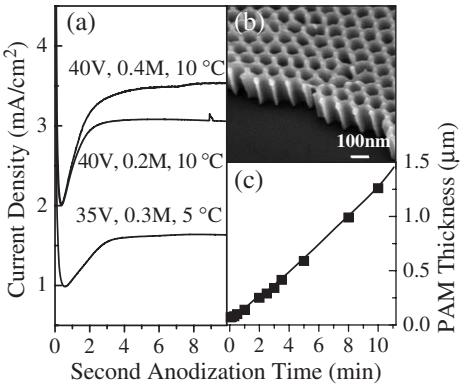

Fig. 2. (a) The current–time characteristics under different anodization voltages, concentrations and temperatures of the electrolyte. (b) A typical FE-SEM image of PAM with thickness of ~150 nm and pore diameter of ~70 nm. (c) The dependence of the PAM thickness on the anodization time under the second anodization conditions of 10 °C, 40 V and 0.3 M $H_2C_2O_4$. The filled squares are the experimental data from the FE-SEM images, and the solid curve is the theoretical results from the current–time characteristics.

density changes with the time as unsteady states, in contrast to the steady state in which the current density is basically constant. During the second anodization, the half-sphere pre-patterns on the Al surface gradually transform from V-shape nanopores at the unsteady states into normal U-shape nanopores at the steady state. Fig. 2(b) shows the typical field-emission scanning electron microscope (FE-SEM, Philips Sirion 200 with a spatial resolution of 2 nm) image of the U-shape PAM with a thickness of ~150 nm, fabricated under the conditions of 10 °C, 40 V, 0.3 M $H_2C_2O_4$ and 1.5 min.

For thick PAMs (>10 μm), the theoretical thickness was suggested to be proportional to the product of the current density (i) and anodization time (t) [8]. However, for ultrathin PAMs (<1 μm), the anodization time is usually less than 10 min, and the current density changes rapidly during the unsteady states. The theoretical thickness (h_{ox}) of the ultrathin PAMs is expected to follow the integrated form of $h_{ox} = k\int_0^t i dt$ with k a constant, while the experimental thickness can be estimated from the FE-SEM images. It is clear that the theoretical thickness h_{ox} can well explain the yielded thickness of the ultrathin PAMs throughout the experimental anodization time with k of $(5.91 \pm 0.02) \times 10^{-8}$ cm^{-3} mA^{-1} s^{-1} as shown in Fig. 2(c). In addition to the anodization time control of the ultrathin PAM thickness, the current density can also be adjusted by the proper operating temperature, anodization voltage, and electrolyte concentration during the ultrathin PAM fabrication as shown in Fig. 2(a). The current density decreases with the operating temperature, anodization voltage and concentration of the electrolyte. However, according to our experimental results, the effect of temperature or anodization voltage changes on the current density is much larger than those of the electrolyte concentration. In a word, we can control the PAM thickness by adjusting the anodizing time and current density.

In terms of obtaining throughout free-standing ultrathin PAMs with controllable diameters, it is well known that free-standing thick PAMs are easy to be prepared while ultrathin PAMs are fragile and hard to be fabricated. Although the $CuCl_2$-based erosive solution was also reported to remove the aluminum [9], so far it has never been reported that the free-standing ultrathin PAMs with the thickness less than 1 μm were obtained without $HgCl_2$ solution. Here, we propose to employ a nontoxic mixture solution of saturated $CuSO_4$ and HCl to remove the Al substrates for free-standing ultrathin PAMs by the aid of a plastic strainer with the height of 1.0 mm, pore diameter of 1.5 mm, and pore distance of 1.0 mm. The PAMs with the unoxided aluminum at the bottom were laid on the plastic strainer, which was fixed in a glass vessel with the surface of the erosive solution just over the top of the strainer. The aluminum reacted drastically with the erosive solution and the aluminum of 0.2 mm in thickness was removed clearly within 2 min while the PAM was intact. The pore diameters of the PAMs are also controllable between 50 and 90 nm through different erosion times in the 5% H_3PO_4 at 30 °C for 30–60 min, at the same time the barrier layers are removed and throughout ultrathin PAMs are obtained.

We have successfully fabricated nc-Si:H AQDs by means of the PECVD under the same deposition conditions of nc-Si:H films by the aid of the highly ordered PAMs with controllable thickness and pore diameter. Fig. 3 displays the morphology of the obtained nc-Si:H AQD arrays with different diameters after removing the PAM masks in a 10% HF at 20 °C for 10 min. The average diameters of the nc-Si:H AQDs in Fig. 3(a) and (b) are ~50 nm and 90 nm, respectively. In each AQD in Fig. 3(a) and (b), there are more than 120 and 360 Si NQDs, respectively. The nc-Si:H AQD and Si NQD sheet densities are thus in excess of 1×10^{10} cm^{-2} and 3×10^{11} cm^{-2}, respectively, comparable to those from the Stranski–Kranstanov mode growth. Based on the above arguments, we can draw a conclusion that highly ordered nc-Si:H AQD arrays can be fabricated with tunable size by the present convenient and low-cost fabrication technique (PAMs in conjunction with the PECVD). The combination of the AQD fabrication through PAM masks with the Si NQDs in nc-Si:H provides us an easy and practical way for the realization of nc-Si:H based nanodevice arrays with true quantum size effects.

Finally, it is interesting to explore the effect of pore size and template thickness on the growth process. The highly ordered nc-Si:H AQD arrays in Fig. 3(a) and (b) are fabricated under the PAMs with only ~150 nm in thickness. The diameters of

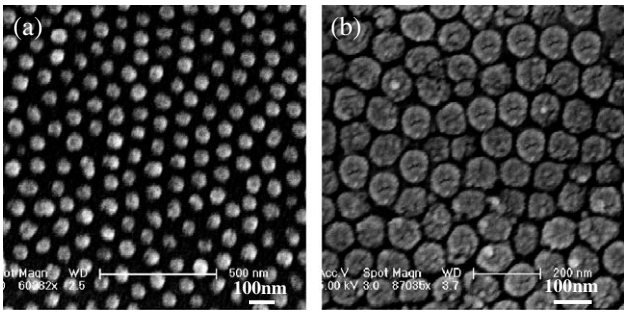

Fig. 3. FE-SEM images of the nc-Si:H AQD arrays with different dot diameters of (a) ~50 nm and (b) ~90 nm.

nc-Si:H AQDs are determined by the pore diameters of the PAMs, i.e., the diameters of nc-Si:H AQDs are basically equal to the pore diameters of the PAMs. Nevertheless, when the PAM thickness is about 300 nm, nc-Si:H AQDs with the size of ~50 nm can be fabricated under large pore diameter PAMs (~90 nm), while no nc-Si:H AQDs were found with small pore diameter ones (~50 nm). With the further increase in the PAM thickness of over 500 nm, no nc-Si:H AQDs can be found on the Si substrates after the PAMs are removed, no matter what the pore diameters are. It is found that large pore size and thin template will help the deposition of the nc-Si:H AQDs through the PAM nanochannels, and the thinner the PAMs are, the more regular the obtained nc-Si:H AQD arrays are.

4. Conclusions

In summary, on the basis of realizing nc-Si:H thin films with very small Si NQDs, highly ordered nc-Si:H AQD arrays have been fabricated on Si substrates by the aid of ultrathin PAMs. The thickness and pore diameter of controllable PAMs play an important role in the fabrication process, and the obtained nc-Si:H AQDs have a tunable diameter from 50 to 90 nm, together with sheet densities of over 1×10^{10} cm^{-2} and 3×10^{11} cm^{-2} for the nc-Si:H AQDs and Si NQDs, respectively. This simple, low-cost and effective approach opens the possibility of creating semiconductor nanodevice arrays, where the Si NQDs will play a key role in the quantum size effects, while the spacing of the uniform AQDs acts as a good electrical insulation.

Acknowledgments

This work was supported by the Natural Science Foundation of China under contract No. 10125416, the Shanghai Major Project of 03DJ14003, and the Shanghai Nanotechnology Fundamental Research Project of 0352nm013.

References

[1] Y.L. He, G.Y. Hu, M.B. Yu, M. Liu, J.L. Wang, G.Y. Xu, Phys. Rev., B 59 (1999) 15352, (and the references therein).
[2] E.H. Nicollian, R. Tsu, J. Appl. Phys. 74 (1993) 4020.
[3] X.Y. Chen, W.Z. Shen, Appl. Phys. Lett. 85 (2004) 287.
[4] H. Chik, J.M. Xu, Mater. Sci. Eng., R Rep. 43 (2004) 103.
[5] X. Mei, D. Kim, H.E. Ruda, Q.X. Guo, Appl. Phys. Lett. 81 (2002) 361.
[6] H. Masuda, K. Fukuda, Science 268 (1995) 1466.
[7] H. Chen, W.Z. Shen, J. Appl. Phys. 96 (2004) 1024.
[8] G. Patermarakis, K. Moussoutzanis, Electrochim. Acta 40 (1995) 699.
[9] T.T. Xu, R.D. Piner, R.S. Ruoff, Langmuir 19 (2003) 1443.